Tellus **000**, 000–000 (0000) Printed 20 September 2012 (Tellus LaTeX style file v2.2)

# How well do state-of-the-art Atmosphere-Ocean general circulation models reproduce atmospheric teleconnection patterns?

## Supplementary Material

By Dörthe Handorf[1⋆], Klaus Dethloff[1],
[1] *Alfred Wegener Institute for Polar and Marine Research, Research Department Potsdam, Telegrafenberg A43, D-14471 Potsdam, German*

20 September 2012

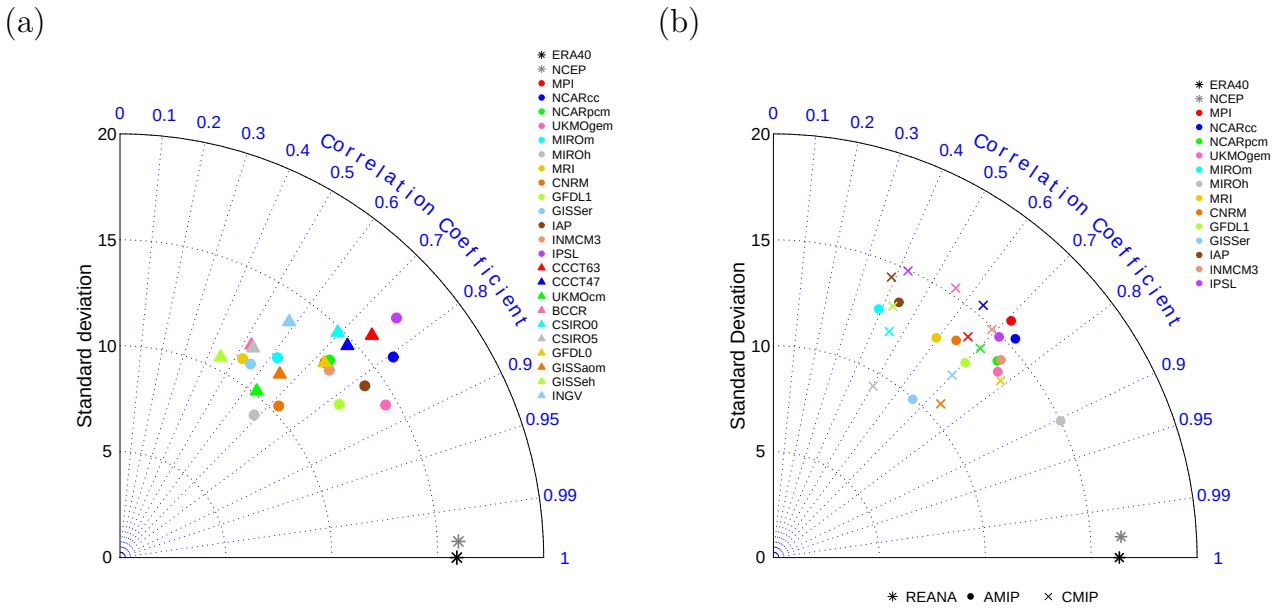


**Figure 1.** Taylor plots for EA/WR of fields of $Z_{500}$ CMIP3/AMIP3 model runs and NCEP/NCAR and ERA40 reanalysis, DJF. (a) CMIP from 1958-1999, (b) CMIP/AMIP from 1979-1999.

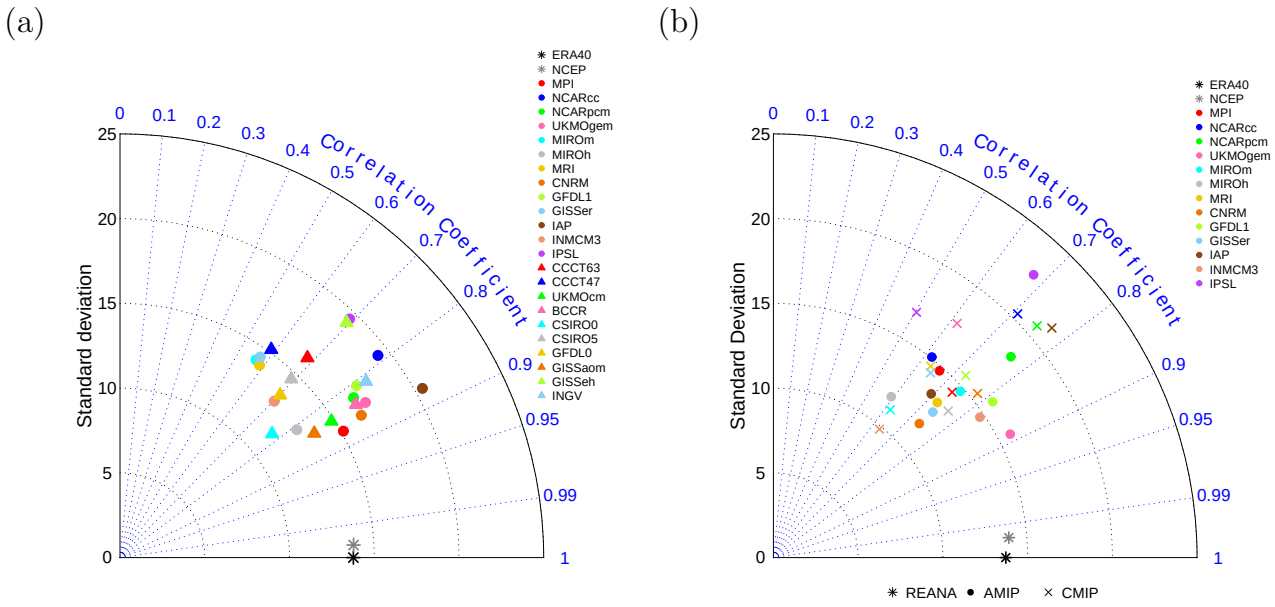


**Figure 2.** Taylor plots for SCAN of fields of $Z_{500}$ CMIP3/AMIP3 model runs and NCEP/NCAR and ERA40 reanalysis, DJF. (a) CMIP from 1958-1999, (b) CMIP/AMIP from 1979-1999.

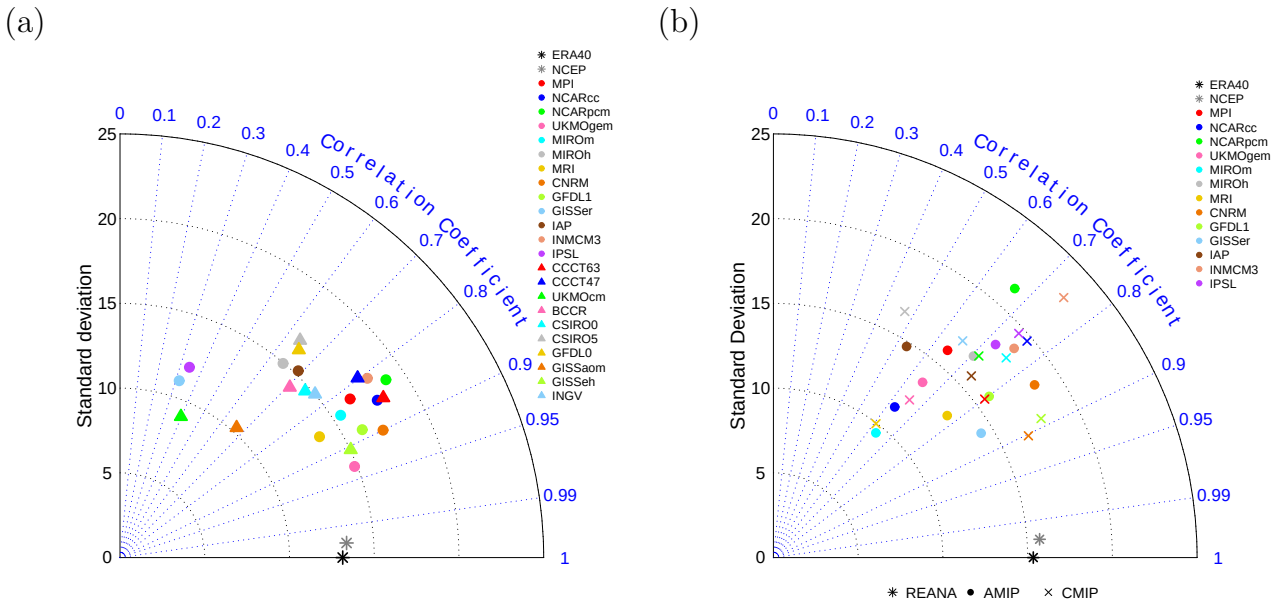


**Figure 3.** Taylor plots for EP/NP of fields of $Z_{500}$ CMIP3/AMIP3 model runs and NCEP/NCAR and ERA40 reanalysis, DJF. (a) CMIP from 1958-1999, (b) CMIP/AMIP from 1979-1999.

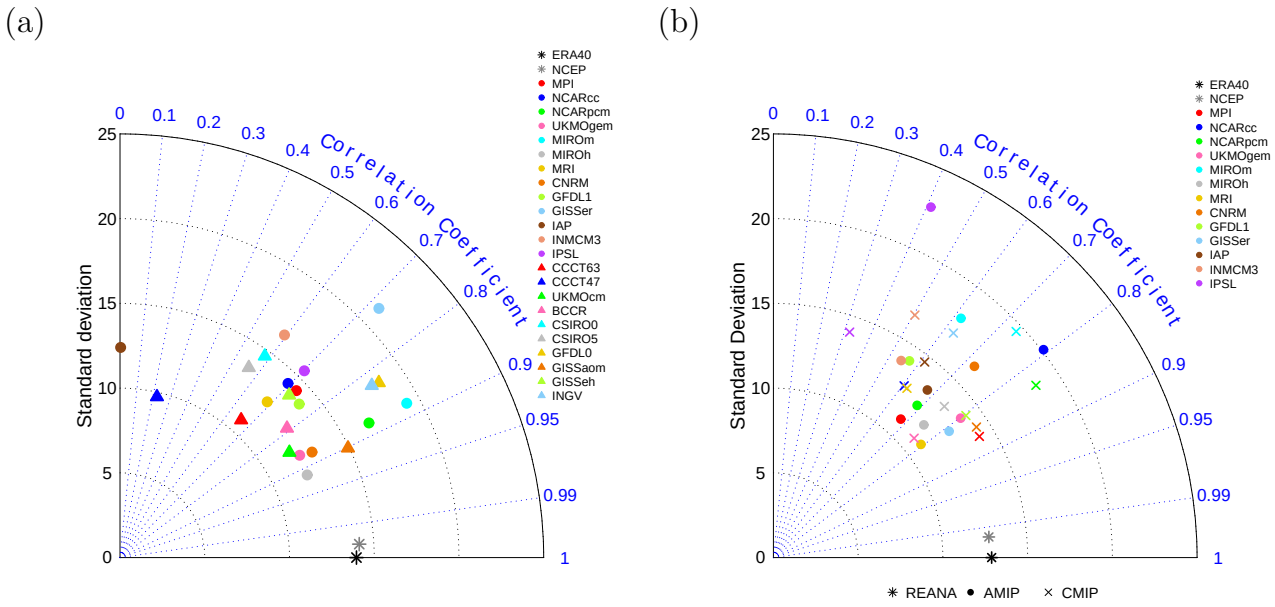


**Figure 4.** Taylor plots for POL of fields of $Z_{500}$ CMIP3/AMIP3 model runs and NCEP/NCAR and ERA40 reanalysis, DJF. (a) CMIP from 1958-1999, (b) CMIP/AMIP from 1979-1999.

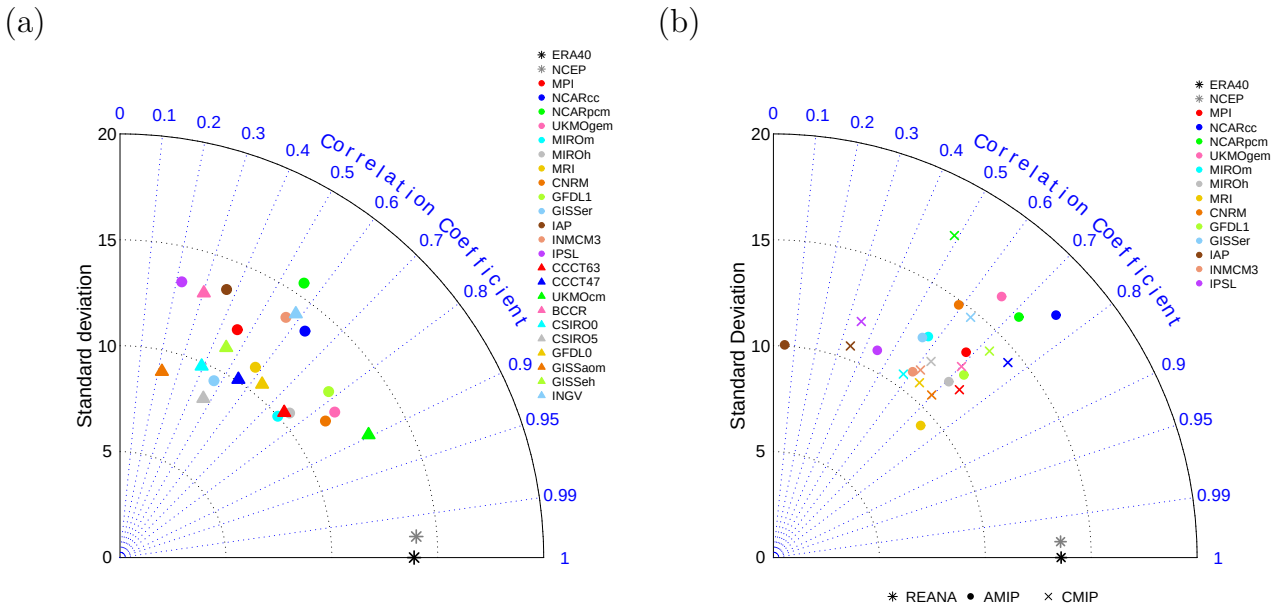


**Figure 5.** Taylor plots for TNH of fields of $Z_{500}$ CMIP3/AMIP3 model runs and NCEP/NCAR and ERA40 reanalysis, DJF. (a) CMIP from 1958-1999, (b) CMIP/AMIP from 1979-1999.

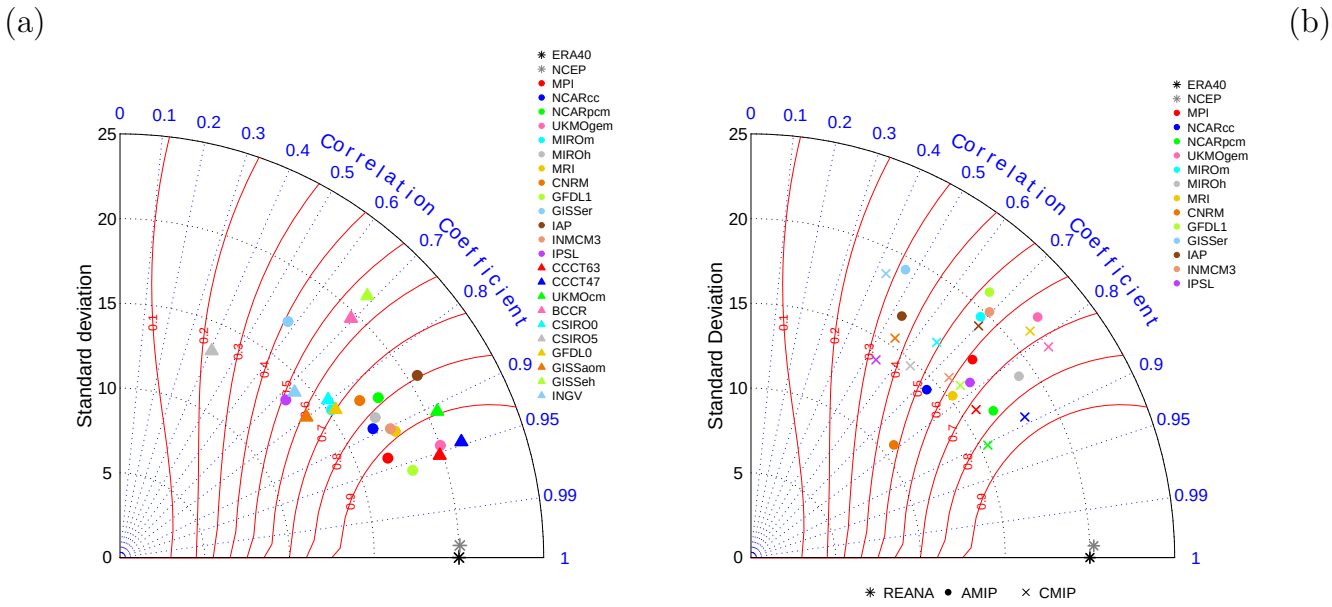


**Figure 6.** Taylor plots for NAO of fields of $Z_{500}$ CMIP3/AMIP3 model runs and NCEP/NCAR and ERA40 reanalysis, DJF. (a) CMIP3 from 1958-1999, (b) CMIP3/AMIP3 from 1979-1999. The red lines are the skill score isolines defined by Eq. 2 with $R_0 = 0.96$ (see Table 3.

(a) (b)

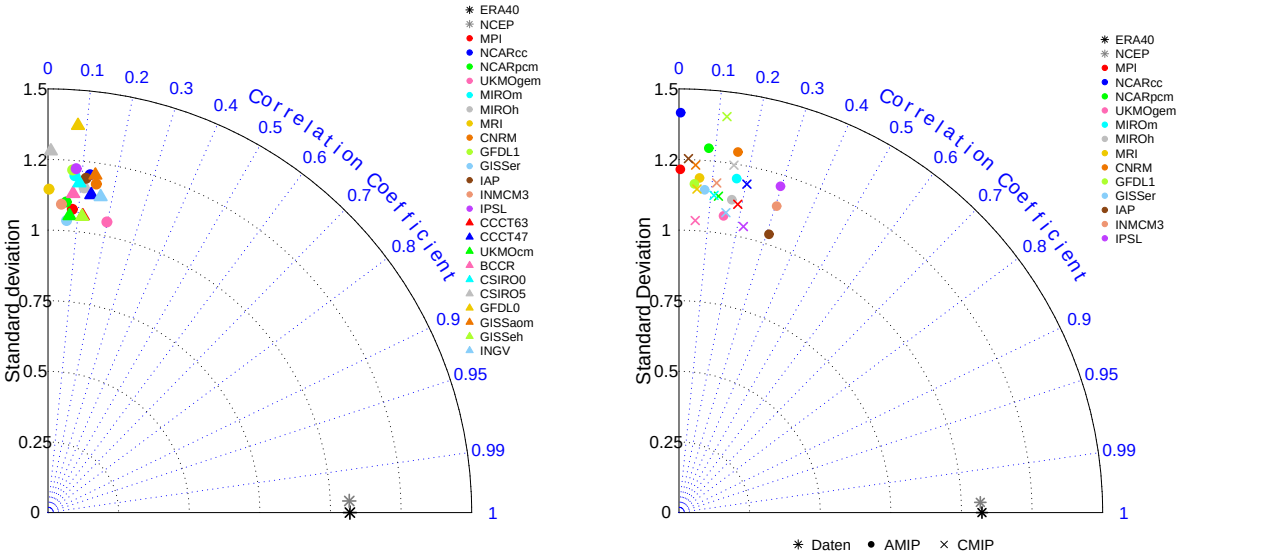


**Figure 7.** Taylor plots for unfiltered time-series of NAO of fields of $Z_{500}$, CMIP3 model runs and NCEP/NCAR and ERA40 reanalysis, DJF. (a) CMIP from 1958-1999, (b) CMIP from 1979-1999, AMIP from 1979-1999.

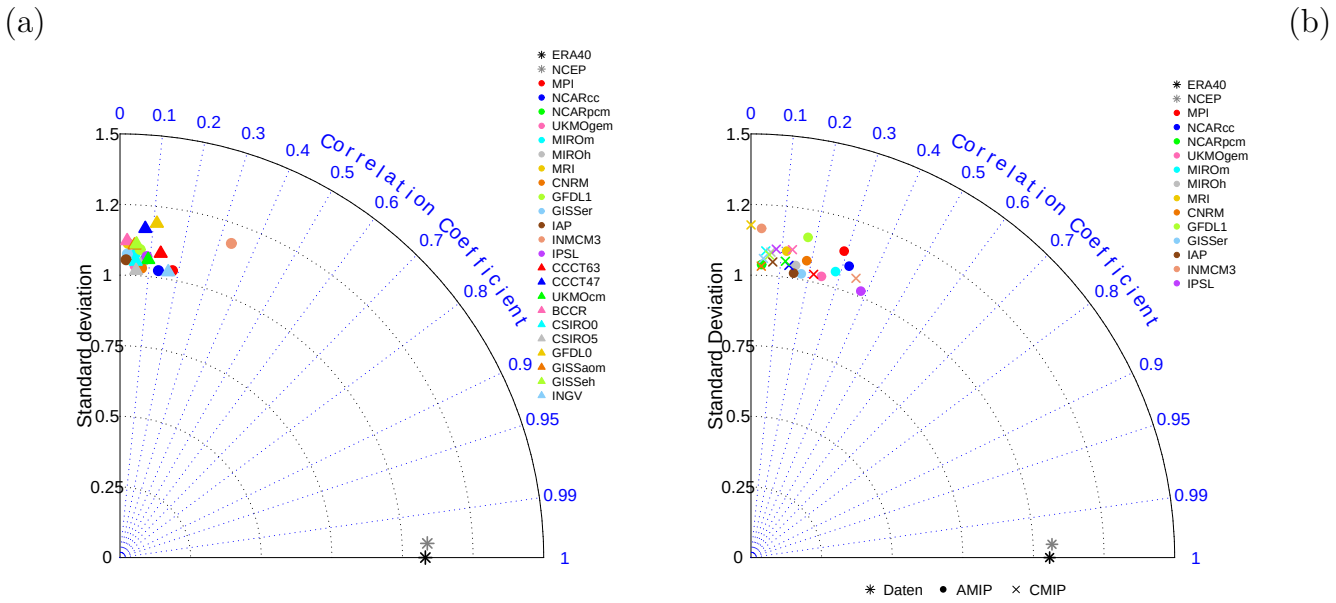


**Figure 8.** Taylor plots for unfiltered time-series of PNA of fields of $Z_{500}$, CMIP3 model runs and NCEP/NCAR and ERA40 reanalysis, DJF. (a) CMIP from 1958-1999, (b) CMIP from 1979-1999, AMIP from 1979-1999.

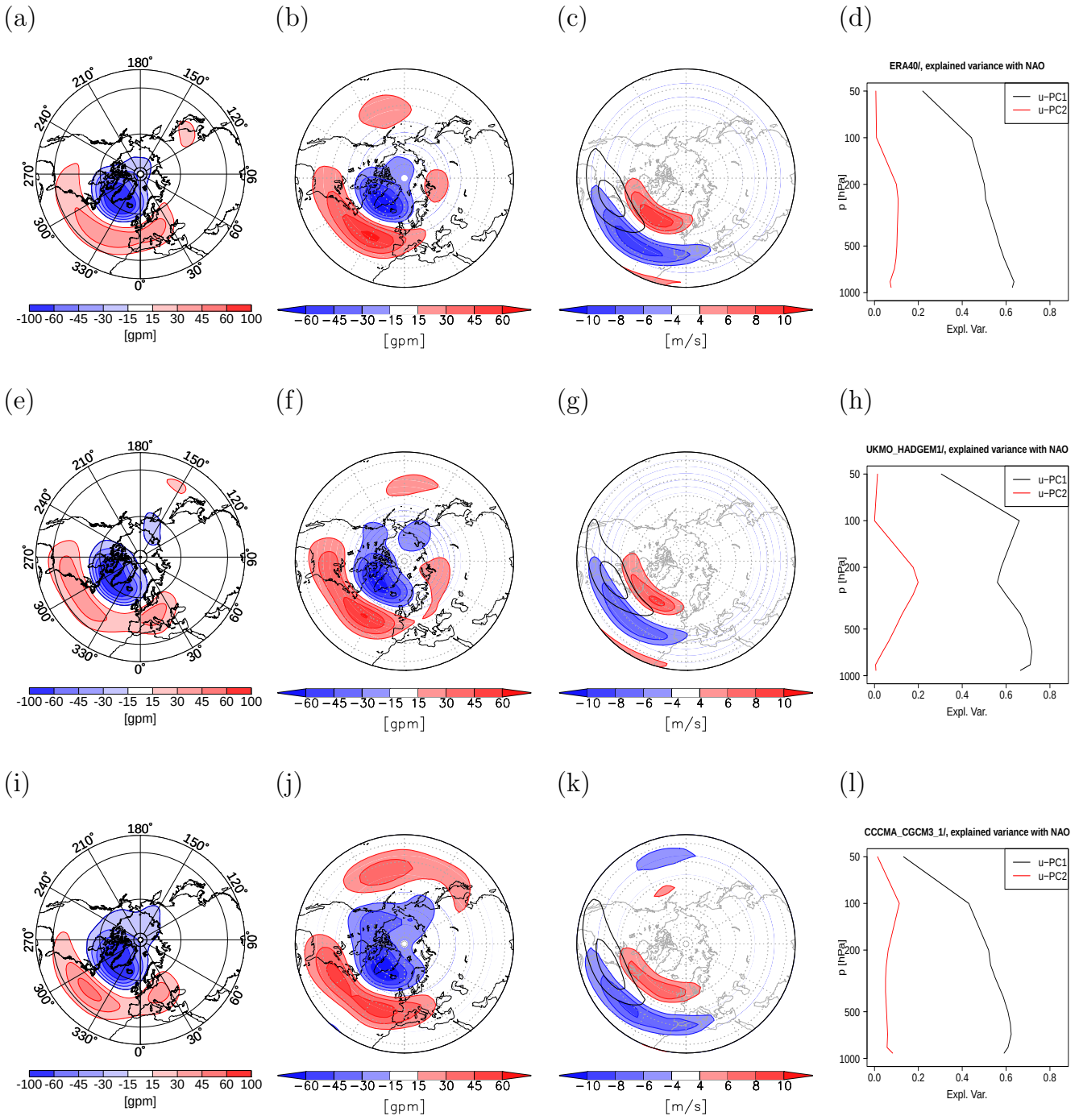


**Figure 9.** Summary of the NAO patterns and their relation to ATL-*u*-EOF1 for ERA40 reanalysis (a-d), UKMO HadGEM1 (e-h), CCCma CGCM3.1 (T47) (i-l). DJF-data from 1958-1999. From left to right: the NAO pattern (a,e,i); the regression pattern of the global geopotential height field at 500hPa onto ATL-*u*-PC1 at 250hPa (b,f,j); the regression pattern of the global zonal wind field at 250hPa onto ATL-*u*-PC1 at 250hPa (colours with overlaid Atlantic mean jet) (c,g,k); the vertical profile of explained variance between the NAO-index and the sectoral ATL-*u*-PC1 at each height (d,h,l).

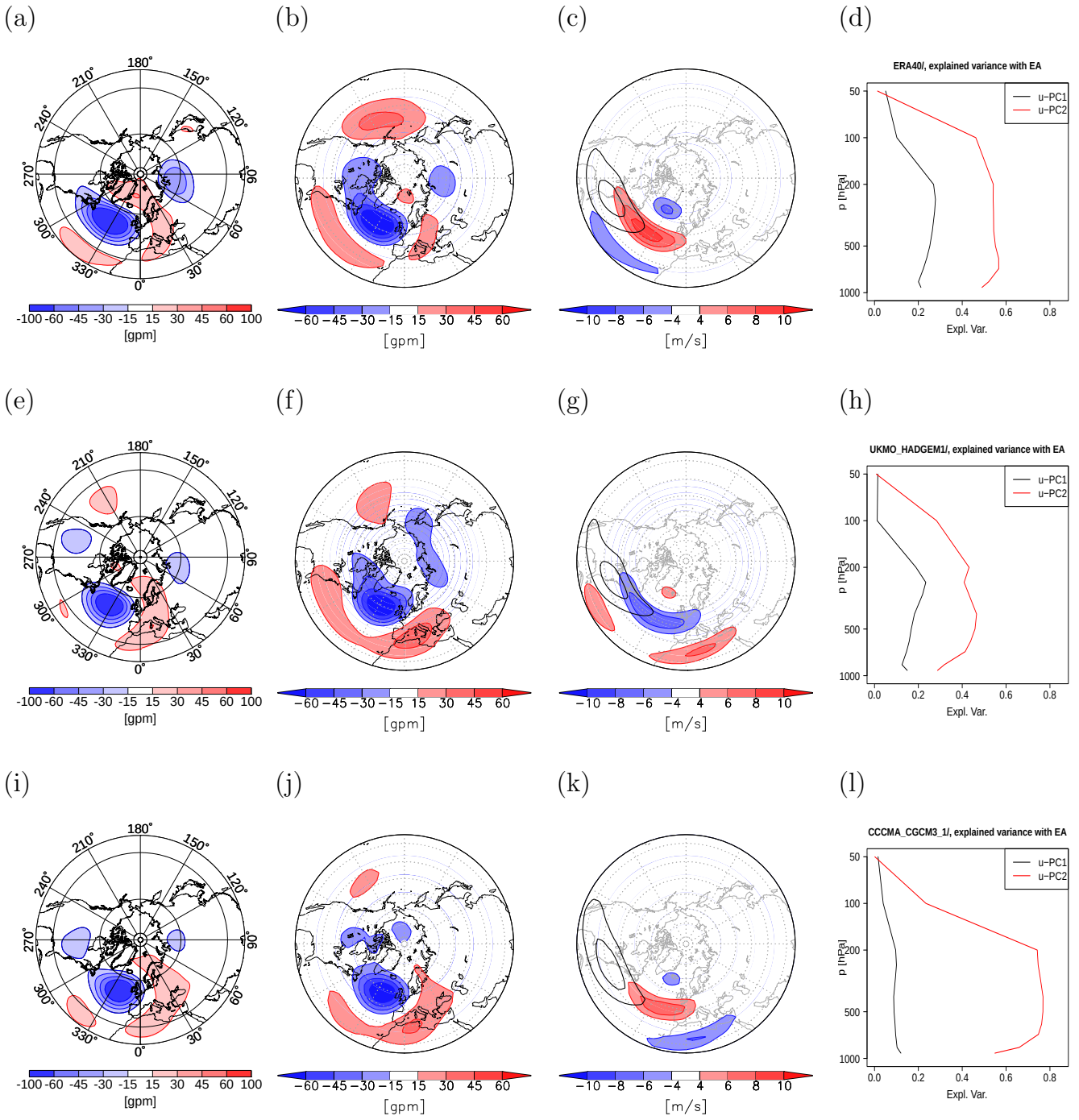


**Figure 10.** Summary of the EA patterns and their relation to ATL-*u*-EOF2 for ERA40 reanalysis (a-d), UKMO HadGEM1 (e-h), CCCma CGCM3.1 (T47) (i-l). DJF-data from 1958-1999. From left to right: the EA pattern (a,e,i); the regression pattern of the global geopotential height field at 500hPa onto ATL-*u*-PC2 at 250hPa (b,f,j); the regression pattern of the global zonal wind field at 250hPa onto ATL-*u*-PC2 at 250hPa (colours with overlaid Atlantic mean jet) (c,g,k); the vertical profile of explained variance between the EA-index and the sectoral ATL-*u*-PC2 at each height (d,h,l).

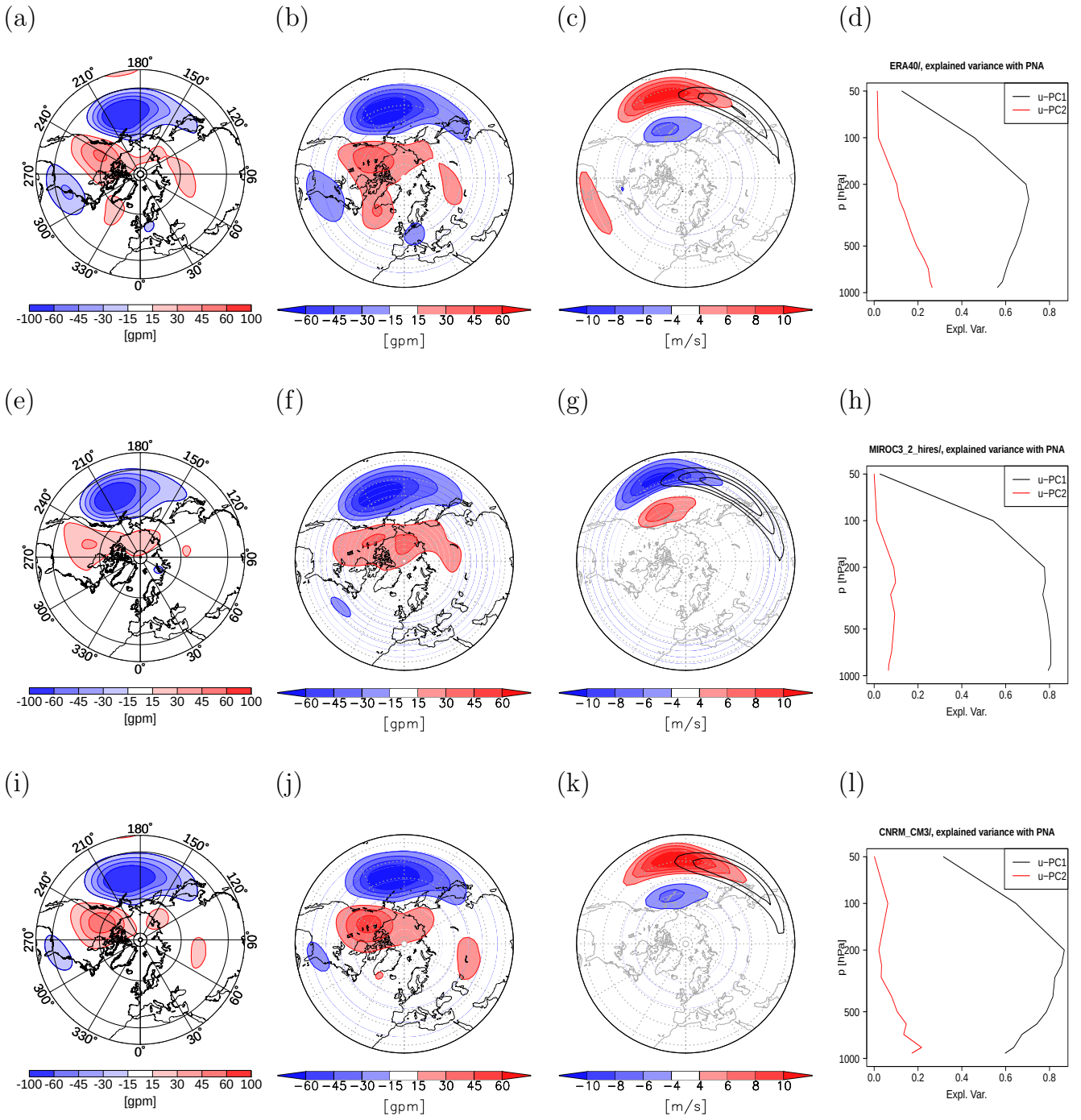


**Figure 11.** Summary of the PNA patterns and their relation to PAC-*u*-EOF1 for ERA40 reanalysis (a-d), MIROC3.2(hires) (e-h), CNRM-CM3 (i-l). DJF-data from 1958-1999. From left to right: the PNA pattern (a,e,i); the regression pattern of the global geopotential height field at 500hPa onto PAC-*u*-PC1 at 250hPa (b,f,j); the regression pattern of the global zonal wind field at 250hPa onto PAC-*u*-PC1 at 250hPa (colours with overlaid Pacific mean jet) (c,g,k); the vertical profile of explained variance between the PNA-index and the sectoral PAC-*u*-PC1 at each height (d,h,l).

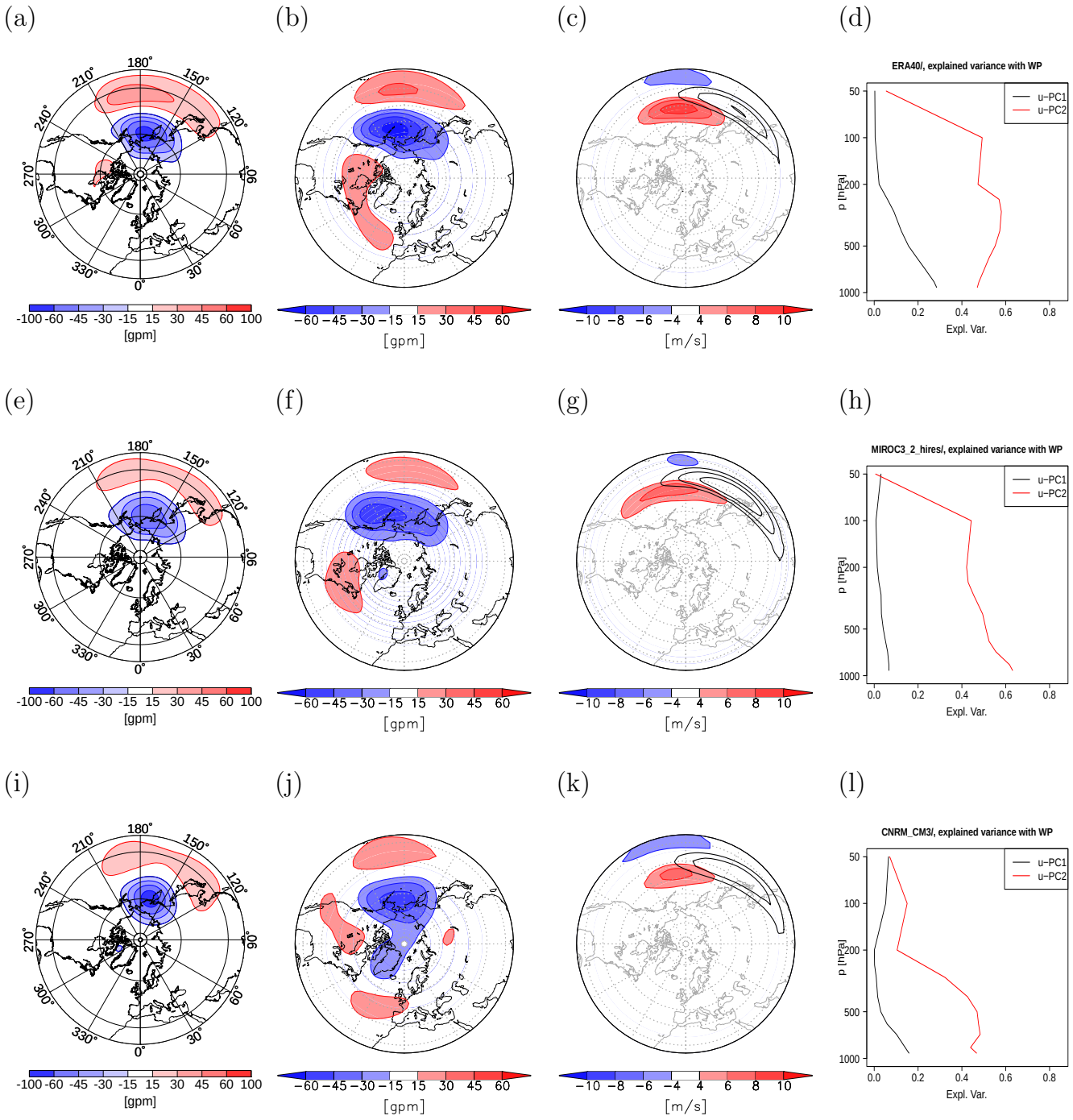


**Figure 12.** Summary of the WP patterns and their relation to PAC-*u*-EOF2 for ERA40 reanalysis (a-d), MIROC3.2(hires) (e-h), CNRM-CM3 (i-l). DJF-data from 1958-1999. From left to right: the WP pattern (a,e,i); the regression pattern of the global geopotential height field at 500hPa onto PAC-*u*-PC2 at 250hPa (b,f,j); the regression pattern of the global zonal wind field at 250hPa onto PAC-*u*-PC2 at 250hPa (colours with overlaid Pacific mean jet) (c,g,k); the vertical profile of explained variance between the WP-index and the sectoral PAC-*u*-PC2 at each height (d,h,l).